Effects of changing roughness on acoustic scattering: (1) natural changes

K. B. Briggs,[1] K. L. Williams,[2] M. D. Richardson,[1] D. R. Jackson[2]

[1] Naval Research Laboratory, Seafloor Sciences Branch, Stennis Space Center, MS 39529-5004, USA.
kevin.briggs@nrlssc.navy.mil, Mike.Richardson@nrlssc.navy.mil
[2]Applied Physics Laboratory, University of Washington, Seattle, WA 98105, USA.
williams@apl.washington.edu, drj@apl.washington.edu

Abstract

High resolution (~0.1-1 cm) measurements of seafloor roughness with underwater stereo photogrammetry were performed during the shallow-water SAX99 acoustic experiment. Changes in morphology due to hydrodynamic and biological processes were observed, and documented by changes in the values of measured slope and spectral strength of the seafloor roughness power spectrum. Roughness spectral and geoacoustic parameters were used in the first-order perturbation model to make backscatter predictions, which were compared with measured acoustic data.

1. Introduction

During the Sediment Acoustics Experiment in the fall of 1999 (SAX99), hydrodynamic and biological processes visibly modified the sea floor. From the outset we were specifically interested in how roughness of the sediment-water interface affected high frequency acoustic scattering from and penetration into the sea floor. Hence, the seafloor roughness was measured in ensonified areas at various times during the experiment to document quantitatively the features created and destroyed by wind-wave currents and benthic animals.

Measurement of seafloor roughness has been an essential task in characterizing parameters controlling high frequency bottom backscattering for a number of acoustic experiments [1-5]. Acoustic scattering is sometimes ascribed to anisotropic roughness in the form of current or wind-wave-generated ripples, a common and prominent feature of shallow-water sea floors. Biogenic roughness features in the form of a generally isotropic distribution of mounds, trails and pits may also be responsible for increased high frequency acoustic scattering, or may diminish scattering through the degradation and smoothing of larger features.

The size and spacing of seafloor roughness features are often characterized by the slope and intercept of the roughness power spectrum [6]. The roughness spectral exponent and intercept of the sea floor have been recognized as significant parameters controlling acoustic backscattering in sandy sediments by acoustic modelers [3, 4]. We present 1-dimensional roughness power spectra and their statistical representations for the SAX99 site based on stereo photographic images collected from 5 October to 5 November 1999, correlate the features with environmental processes acting on the sea floor, and compare the measured acoustic backscattering strength with that predicted by the composite roughness model using the statistical roughness parameters.

2. Methods

2.1 Stereo photogrammetry

Stereo photography was conducted with a diver-operated 35 mm underwater stereo camera attached to a PVC frame. Two Nikon 28 mm water-corrected lenses were separated by 61 mm in the Photosea stereo camera, yielding a 55 cm × 72 cm photographic overlap area when the camera is placed 91 cm above the seafloor. The area of the bottom to be photographed was illuminated with a 150 J Photosea underwater strobe mounted in the diver-operated system. Stereo photographs were analyzed by digitizing roughness height values at regularly spaced intervals (0.105 cm) using a Benima (Hasselblad) AB photogrammetric stereocomparator. The photogrammetric software provided by Benima corrected the measurements for distortion caused by refraction in sea water and lens aberrations. Use of the stereo comparator allowed for high frequency sampling of bottom roughness with a horizontal accuracy of nearly 0.01 mm. Three profiles approximately 54 cm long were digitized from each of the stereo photographic images. Orientation of the three profiles was established in each case as parallel to the azimuth of the transmitted acoustic energy. At one particular site, successive, overlapping stereo images were joined by ending and beginning successive digitizations at easily recognizable features on the sea floor, resulting in extended profiles of up to 3.5 m long [6, 7].

The roughness profiles were evaluated for height fluctuations as a function of spatial frequency with the

TG Leighton, GJ Heald, HD Griffiths, G Griffiths, (eds.), 'Acoustical Oceanography', Proc. Institute of Acoustics Vol. 23 Part 2, 2001.

roughness power spectrum estimator suggested by D. Percival of the Applied Physics Laboratory-University of Washington. The digitized data (512 equally spaced height measurements) were prewhitened by taking differences of adjacent data points, and then the possible leakage was eliminated by subtracting the sample mean from the prewhitened data. The resultant data were tapered with a 20 percent cosine bell taper. A fast Fourier transform was applied to compute a periodogram, which was subsequently corrected for prewhitening by dividing each spectral value by $4\sin 2\pi f_j \Delta$, where f_j is defined by $j/N\Delta$, $j = 0, 1, 2, \ldots N/2$, and Δ is the digitizing interval. Periodograms were smoothed by the ensemble averaging of spectra derived from digitized data collected from the same site, orientation and date. The pre-processing removed artifacts created by truncated data sets.

Wave height and period were measured with a bottom-mounted Parascientific digiquartz pressure transducer. Pressure fluctuations were measured at 4 Hz from 18-19 meters water depth. A noise floor as a result of the 19 m water depth limited detection of wave periods to those greater than 6 seconds.

Acoustic backscatter was measured with the Benthic Acoustic Measuring System (BAMS), a bottom-mounted, autonomous system operating from a tripod frame, which scans the sea floor with a 40 kHz transducer rotating in the horizontal plane. Scattering was also measured at 10–150 kHz with the Sediment Transmission Measurement System (STMS) at a site located 200 m east of the BAMS site.

The model used to make predictions from the geoacoustic and roughness data is described by Jackson *et al.* [4]. The input parameters are sediment sound speed ratio, density ratio, sound speed attenuation, density correlation length, roughness spectral exponent and strength.

3. Roughness measurements

Initial seafloor roughness measurements were made at the BAMS site on 5 Oct. 1999 before deployment of the acoustic towers. The sea floor was characterized by relatively sharp-crested, well developed storm ripples (Figure 1). The bedforms had wavelengths of approximately 50 cm and the crest-to-crest orientation was roughly north-south. An average slope of –3.16 was calculated from regressions of roughness variance against spatial frequency. This value was determined by a combination of very little high-spatial-frequency roughness and significant low-spatial-frequency roughness (Figure 2).

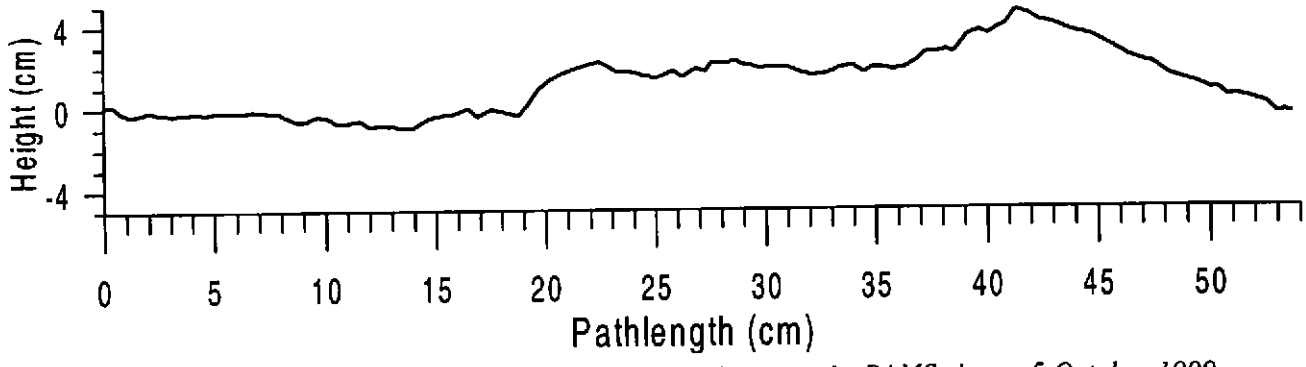

Figure 1. Two-dimensional profile of seafloor roughness at the BAMS site on 5 October 1999.

Site	Date	Elapsed time *re* storm event (d)	Azimuth of profile	Spectral slope	Spectral intercept (cm^3)
BAMS	5 Oct.	-3	N	-3.16	0.00064
	19 Oct.	10	N	-2.73	0.00096
	23 Oct.	14	NNE	-2.54	0.00077
	5 Nov.	27	NNE	-2.53	0.00071
STMS	4 Nov.	26	NNE	-2.44	0.00117
	4 Nov.	26	SE	-2.47	0.00126

Table 1. Roughness power spectrum slopes and intercepts as functions of time. A major storm event occurred on 8-9 October and elapsed time is relative to the event.

A significant storm event occurred on 8-9 October (Figure 3), building new bedforms at a new orientation (ripples facing NNW). Following the storm event, the ripples decayed primarily from biogenic activity that initially tends to smooth sharp features and decrease bedform height and ultimately result in random, isotropic roughness. After ten days of benign oceanographic conditions the average roughness power spectrum had a slope

of –2.73 due to subdued ripple heights and a spectral strength (intercept) value of 0.0096 due to an increase in small-scale roughness (Table 1). By 23 October the ripples decayed even more, resulting in less steep slopes due to flattening of ripples to subtle undulations (Figs. 4 and 5). Nearly four weeks after the storm event (and 2 days since a lesser event on 1-3 November), the ripple decay stabilized, exhibiting little change in slope or intercept in the last 13 days.

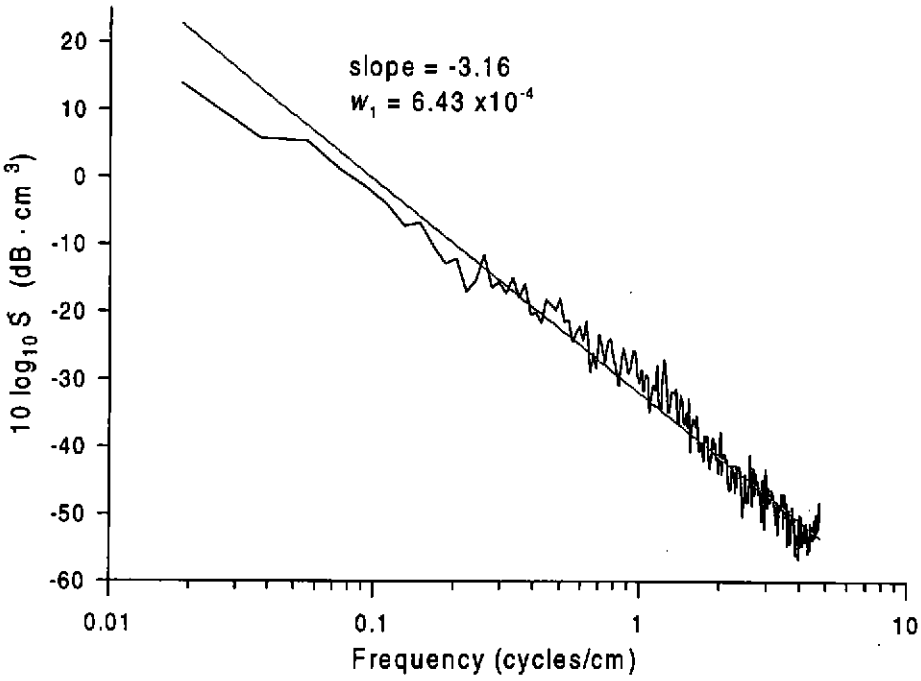

Figure 2. 1-D roughness power spectrum estimated for the BAMS site on 5 October 1999

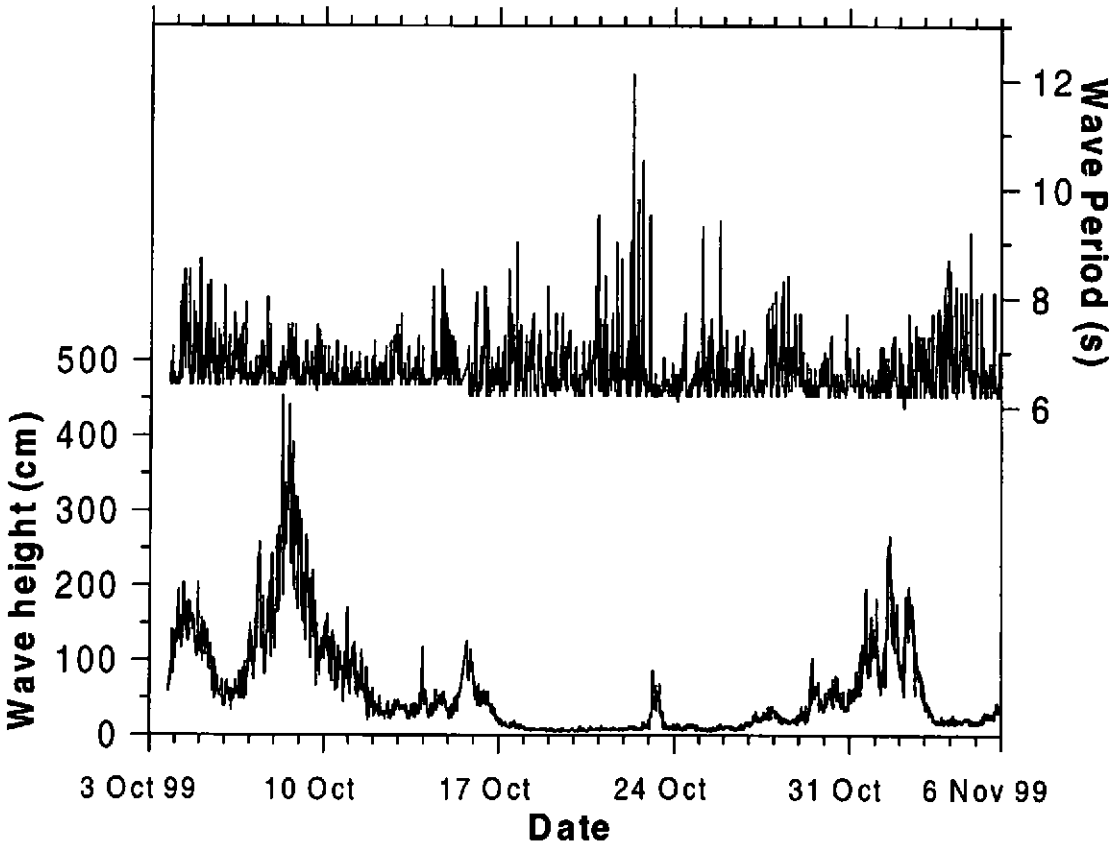

Figure 3. Wave height and period measured by the pressure sensor on the ADP. Change in baseline in wave period data is due to the re-location of instrument on 15 October.

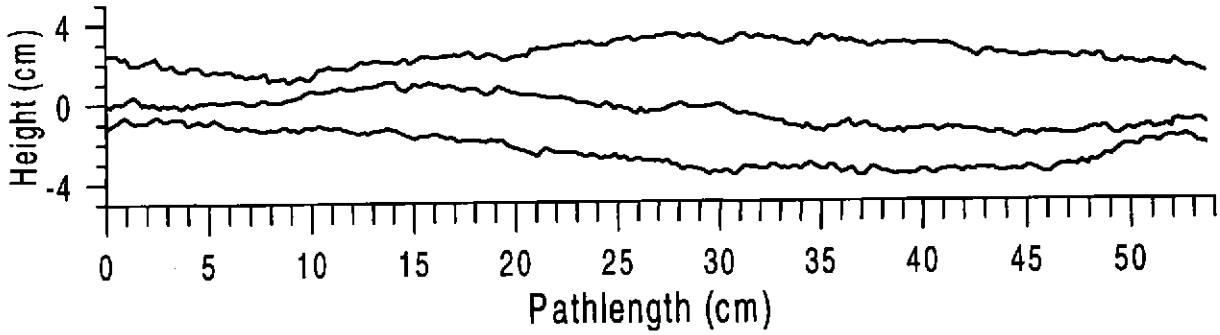

Figure 4. Three 2-dimensional profiles of seafloor roughness at the BAMS site on 23 October 1999.

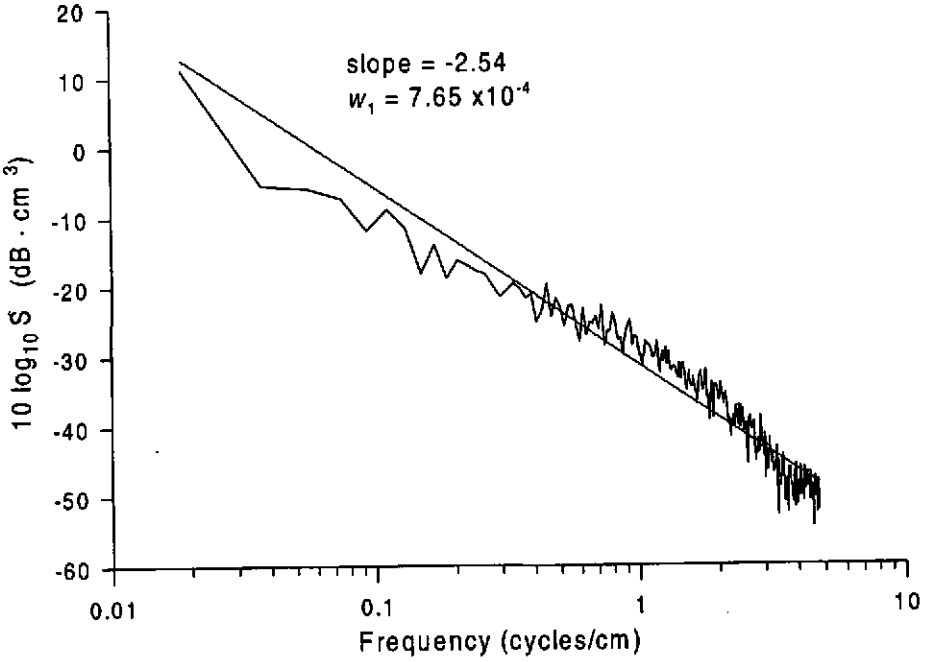

Figure 5. 1-D roughness spectrum estimated for the BAMS site on 23 October 1999.

A short distance from the BAMS site, but closer to the ship at anchor, the STMS site had subtly different features (though not statistically different). At 26 days elapsed time from the storm event the average roughness power spectrum at the STMS site had a decayed spectral slope (-2.44), but considerable small-scale roughness indicated by a relatively high spectral strength value (0.00117). The similar spectral slope values derived from nearly orthogonal-oriented spectra indicate that the roughness was nearly isotropic on 4 November.

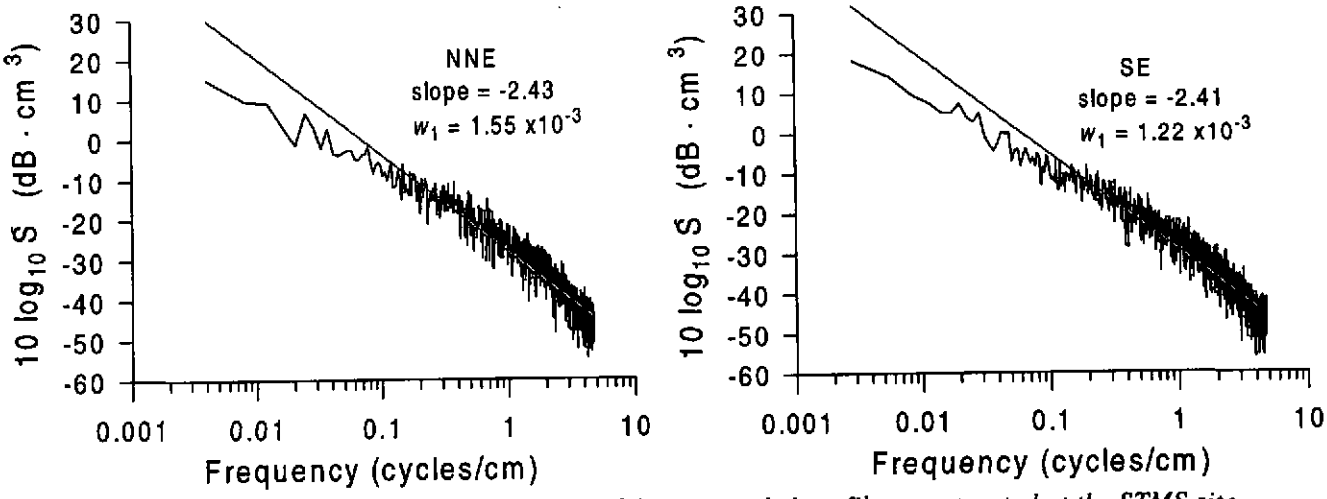

Figure 6. Roughness power spectra generated from extended profiles constructed at the STMS site.

Larger-scale roughness with overlapping profiles was measured at the STMS site on 4 November. Despite attaining extended profiles of 2.5 to 3.5 m, the roughness spectral slopes were similar to the slopes estimated from the constituent shorter profiles (Figure 6). The low frequency portion of the spectra (0.004 to 0.1 cycles/cm), however, has a slope that is definitely less steep than the high frequency portion of the spectra.

4. Model-data comparisons

First-order perturbation theory [4] was employed to make predictions at 40 kHz using the roughness spectral parameters and the input parameters in Table 2. The slope of the roughness spectrum, however, is an average of the spectrum's behavior over several decades of spatial frequency. The slope and intercept values depend on which spatial frequency decade is included in the regression. Hence, roughness spectrum parameters are chosen from the 0.2 to 2.0 cm^{-1} decade in Table 3 in order to include the wavenumber corresponding to 40 kHz. The values in Table 2 are derived from geoacoustic measurements made from diver cores or an *in situ* measurement system (38 kHz) in the case of compressional wave speed and attenuation. Diver cores were sectioned at 2 cm intervals for sediment density analysis after being acoustically logged at 1 cm increments at 400 kHz. Average values for sound speed and attenuation are determined from *in situ* measurements at 38 kHz, whereas variance and correlation estimates are calculated from 400 kHz fluctuations. Density spectral strength is calculated from the density variance and the density correlation length. The density spectral exponent derived from the exponential covariance is 4. Correlation length is estimated with a first-order autoregressive technique designed for abbreviated datasets and assuming an exponential autocorrelation function [8]. The compressibility fluctuation ratio (μ) is a proportionality factor relating the sound speed fluctuations to density fluctuations in the sediment. More detailed descriptions of the model and its input parameters are presented by Jackson *et al.* [4].

Water *Vp* (m/s)	Compress. Wave Attenuation (dB/m/kHz @ 38 kHz)	*Vp* Ratio	*Vp* Variance	Density Ratio	Density Variance	Density Spectral Strength (cm3)	Density Correlation Length (cm)	Compressibility Fluctuation Ratio (μ)
1535	0.334	1.16	151.57	2.03	2.33×10^{-4}	2.34×10^{-6}	2.39	-2.84

Table 2. Input parameters used in model-data comparisons. Values are averages calculated from 20 cm deep cores. Average compressional wave speed and attenuation were measured with 38 kHz in situ probes; Vp ratio is the ratio of sediment sound speed to water sound speed; density ratio is the ratio of sediment density to water density.

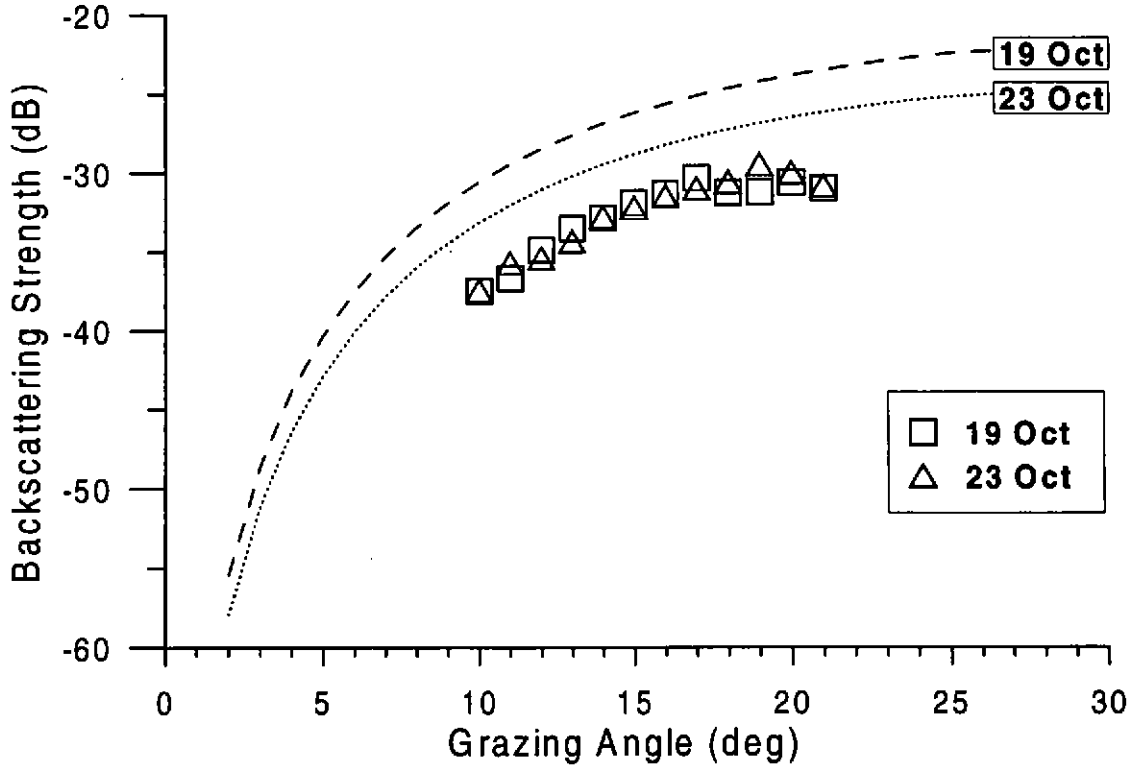

Figure 7. Backscattering strength vs. grazing angle at 40 kHz. Predicted results indicate a decrease in scattering from 19 October to 23 October. Measured results are plotted as symbols.

Although the model predicts about a 2 dB difference in backscatter intensities corresponding to the two different roughness spectra, it overpredicts the measured backscattering intensity by 3 to 6 dB (Figure 7). Furthermore, the measured bottom backscattering is not significantly different on the two dates despite the change in the roughness spectrum indicated in Figure 5. According to the model, roughness scattering levels are greater than volume scattering levels by at least 26 dB over the grazing angle range 2°-30°.

Date	Spatial frequency (cm^{-1})	Spectral slope	Spectral intercept (cm^3)
5 Oct.	0.02 to 5.0	-3.16	0.00064
	0.2 to2.0	-3.01	0.00090
	0.02 to 0.2	-2.57	0.00118
19 Oct.	0.02 to 5.0	-2.73	0.00096
	0.2 to2.0	-2.41	0.00139
	0.02 to 0.2	-2.37	0.00084
23 Oct.	0.02 to 5.0	-2.54	0.00077
	0.2 to2.0	-1.95	0.00119
	0.02 to 0.2	-2.42	0.00033
5 Nov.	0.02 to 5.0	-2.53	0.00071
	0.2 to2.0	-2.16	0.00099
	0.02 to 0.2	-2.00	0.00108

Table 3. Values of roughness spectral slope and intercept for the entire measured spectrum (0.02 to 5.0 cm^{-1}) and the truncated spectra calculated for 4 time periods at the BAMS tower.

It is useful to note that the predicted variation in backscattering strength as a function of time is a function of frequency. For example, if the model were run at 4 kHz, the spectral slope and intercept values from the 0.02 to 0.2 cm^{-1} frequency band would be used and the model would predict a larger difference (about 4 dB) between data acquired on 19 Oct. and on 23 Oct. compared to the predictions at 40 kHz in figure 7.

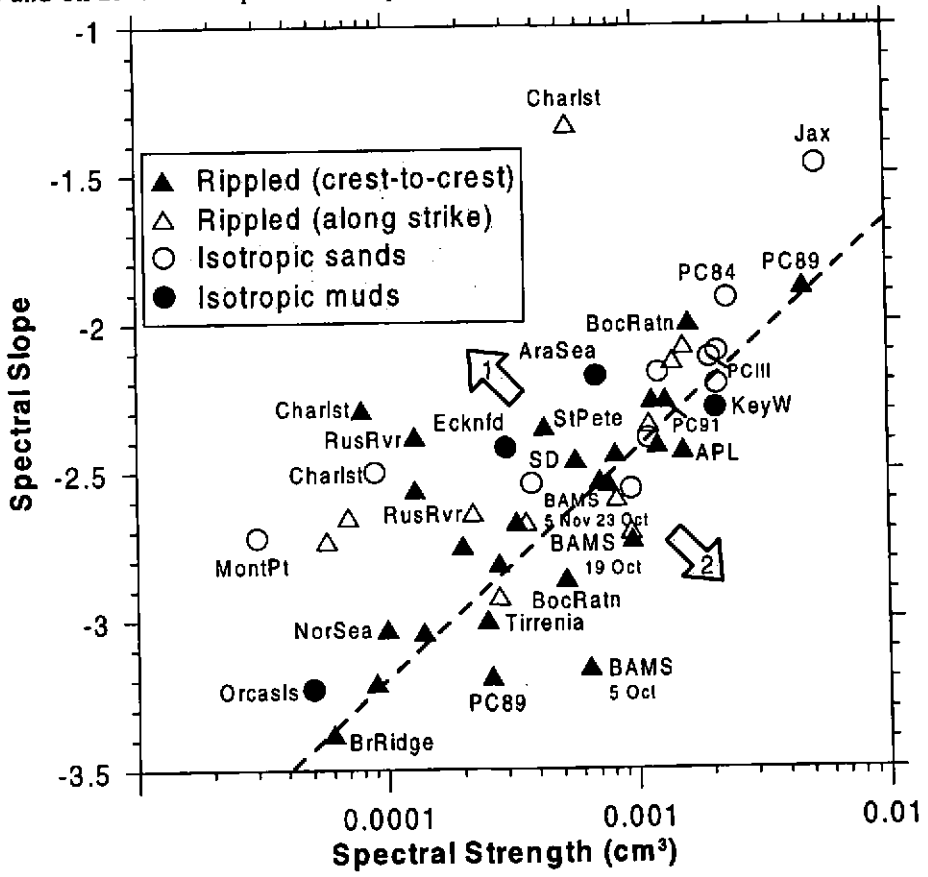

Figure 8. Plot of roughness power spectral slope as a function of roughness power spectral strength for various roughness measurements of shallow-water sea floors. Dashed line represents trend of slope determination essentially by intercept (little or no change in low-spatial-frequency roughness).

5. Conclusions

Roughness power spectra, in terms of the spectral slope and intercept, are useful in describing the salient morphological features of the sea floor. We have demonstrated that the spectral slope and intercept can track changes occurring in a sandy ripple bed as the ripple structure degrades from steep, sharp-crested ripples set up by hydrodynamic stress generated from storms to subtly undulating, nearly isotropic roughness under the influence of bioturbation. Biogenic roughness in this particular experiment is characterized chiefly by high-spatial-frequency fluctuations (surface trails and small feeding pits) in relative sediment height. Little high-spatial-frequency fluctuations, but significant low-spatial-frequency fluctuations (ripple crests and troughs) characterize hydrodynamic roughness. The coincidence of large low frequency roughness and small high frequency roughness of fresh ripple beds results in the steepest slopes; the converse results in the least steep slopes and describes degraded ripples. Though simple in concept, this type of relationship is dependent on environmental variables such as water depth, sediment type, and biological community type.

Plotting spectral slope as a function of the spectral intercept from a compilation of roughness data may indicate important patterns that might help us model roughness scenarios and, ultimately, backscattering from sediment type. Using all the stereo photogrammetric measurements we made on continental shelf sea floors since 1983, roughness spectral slope is plotted against spectral strength in Figure 8. Because spectral slope is related to intercept, we would expect to see a positively sloped trend in the data. The arbitrary dashed line in the figure represents the trend of spectral slope changing as a direct consequence of changes in high-spatial-frequency roughness. That is, little or no change in low-spatial-frequency roughness occurs as the slope changes. Values occurring in the direction of arrow "1" (to the left of the dashed line) represent roughness spectra deviating from the trend by significant *decreases* in low frequency roughness relative to changes in high frequency roughness. Values occurring in the direction of arrow "2" (to the right of the dashed line) represent roughness spectra deviating from the trend by significant *increases* in low frequency roughness relative to changes in high frequency roughness. Examples of an environment represented in the former scenario are muds with little biogenic roughness (Eckernförde Bay, Arafura Sea, Orcas Island) or sands with fully decayed or low relief ripples (Charleston, Montauk Point). Suppositions about seafloor microtopography made from the trends in roughness parameters depicted in Figure 8 are discouragingly few (*e.g.*, isotropic and anisotropic roughness measurements do not segregate). The natural decay of ripple morphology at the BAMS site, however, may be tracked from a point far below the dashed line to right on the dashed line. Longer term decay (months) and an eventual equilibrium between biogenic and hydrodynamic processes may be responsible for the spectral parameters deviating to the left of the trend line.

The data plotted in Figure 8, with the notable exceptions of the BAMS, Russian River, and PC89-91-III measurements, are only an instant temporal sample of a dynamic process. Hence, the lack of definitive trends in roughness among sediment types and roughness orientations may be due to the measurements being temporally uncorrelated. Moreover, the roughness data are restricted spatially compared to the size of an acoustic "footprint". These temporal and spatial limitations of roughness measurements have important implications for their use in acoustic prediction. For instance, interpretation of the offset seen in Figure 7 between acoustic data and model predictions should be approached with caution. The uncertainties in the statistical representation of seafloor roughness (+ 2 dB to −3 dB for the 95% confidence limits) as well as the measured acoustic data (± 2 dB) are such that the data do not necessarily invalidate the model. Furthermore, the predicted difference in scattering from 19 October to 23 October is smaller than the statistical uncertainty in the measured data. The same roughness parameters used with a Biot rather than a fluid approach, however, give a better agreement between measured and predicted data, at least for grazing angles less than 21° [9]. More work is needed to refine the model parameters so as to allow a continued testing of this and alternate acoustic scattering models.

Acknowledgements

This work was supported by the Office of Naval Research and Naval Research Laboratory Program Element 0601153N. The NRL contribution number is AB/7431--00-0010.

References

[1] Stanic S, Briggs KB, Fleischer P, Ray RI and Sawyer WB. Shallow-water high-frequency bottom scattering off Panama City, Florida. *Journal of the Acoustic Society of America* 1988; **83**: 2134-2144

[2] Stanic S, Briggs KB, Fleischer P, Sawyer WB and Ray RI. High-frequency acoustic backscattering from a coarse shell ocean bottom. *Journal of the Acoustic Society of America* 1989; **85**: 125-136

[3] Jackson DR and Briggs KB. High-frequency bottom backscattering: Roughness versus sediment volume scattering. *Journal of the Acoustic Society of America* 1992; **92**: 962-977

[4] Jackson DR, Briggs KB, Williams KL and Richardson MD. Tests of models for high-frequency seafloor backscatter. *IEEE Journal of Oceanic Engineering* 1996; **21**: 458-470

[5] Stanic S, Goodman RR, Briggs KB, Chotiros NP. Shallow-water bottom reverberation measurements. *IEEE Journal of Oceanic Engineering* 1998; **23:** 203-210

[6] Briggs KB. Microtopographical roughness of shallow-water continental shelves. *IEEE Journal of Oceanic Engineering* 1998; **14:** 360-367

[7] Briggs KB and Ray RI. Seafloor roughness power spectra: trends and implications for high-frequency acoustic modeling, in *Shallow-Water Acoustics*, China Ocean Press, Beijing, China, 1997, pp. 347-352

[8] Briggs KB and Percival DB. Vertical porosity and velocity fluctuations in shallow-water surficial sediments and their use in modeling volume scattering, in *High-Frequency Acoustics in Shallow Water*, N. Pace et al. (eds.), NATO SACLANT Undersea Research Centre, La Spezia, Italy, 1997, pp. 65-73

[9] Thorsos EI, Williams KL, Jackson DR, Richardson MD, Briggs KB, Tang D. An experiment in high-frequency sediment acoustics:SAX99, in *'Acoustical Oceanography', Proceedings of the Institute of Acoustics Vol. 23 Part 2, 2001,* T G Leighton, G J Heald , H Griffiths and G Griffiths, (eds.), Institute of Acoustics, (this volume), pp. 344-354.